JOURNAL OF CATALYSIS 130, 52–61 (1991)

# Surface Enrichment in Mixed Oxides of Cu, Co, and Mn, and Its Effect on CO Oxidation

B. L. YANG,[1] S. F. CHAN, W. S. CHANG, AND Y. Z. CHEN

*National Central University, Chemical Engineering Department, Chung-Li, Taiwan, Republic of China*

Received October 2, 1990; revised January 23, 1991

X-ray photoelectron spectroscopy (XPS) and other surface and bulk characterization techniques were employed in the study of mixed oxides of Cu, Co, and Mn as catalysts for CO oxidation. It was found that Mn was enriched at the surface over Cu and Co, and Cu was enriched over Co. XPS data also suggested that the presence of Mn resulted in lowering of the oxidation states of Co and Cu. The difference in CO oxidation activity among different mixed oxides was well explained by the effects of surface enrichment and the change in the oxidation state of surface cations. 

## INTRODUCTION

Mixed oxides of transition metals are important catalysts in both selective oxidation (*1*) and total oxidation (*2, 3*). Very often the catalytic performance of a mixed oxide is found to depend on the composition, the crystal structure, the preparation procedure, and the history of pretreatment of the catalyst. Mixed oxides of transition metals were known to be active in removing CO early in the twenties (*4*). The study was accelerated during World War I under the military need of gas masks. The CO remover developed, Hopcalite, was a mixed oxide of manganese and copper, or further added with cobalt and silver oxides (*4*). However, the lack of basic understanding of catalysis left the so-called "mixture effect" unanswered. Stimulated by their potential uses in catalytic conversion of automotive exhaust, mixed oxides have been systematically studied since the sixties (*5*). The research has become increasingly active in recent years. Two current emphases are to develop contaminant-resistant base metal oxides to replace part of the precious metals presently used in the catalytic converters (*6, 7*), and to develop oxide catalysts with extremely high thermal stability for catalytic combustion (*3*). An encouraging breakthrough in the development of water-resistant low-temperature CO oxidation catalysts has also been reported recently (*8*).

Many studies were aimed to disclose the mixture effect of the mixed oxide catalysts. Early studies found a correlation between the amount of available oxygen and the activity of a mixed oxide (*9, 10*). The importance of crystal structure was later reported. Both spinel (*11, 12*) and perovskite (*13, 14*) materials were found to be especially active. There were also other effects studied, like the support effect (*15*), the interesting effect of surface activation by frictional grinding (*16, 17*), and the poisoning effect (*7, 18, 19*). Only recently were surface characterization techniques like X-ray photoelectron spectroscopy (XPS) and ion scattering spectroscopy (ISS) employed in the study of Hopcalite (*20, 21*). Yoon and Cocke (*20*) employed XPS in the study of a model Hopcalite surface of $CuMn_2O_4$ obtained by controlled oxidation of a Cu–Mn alloy. Veprek *et al.* (*21*) reported a strong enrichment of potassium at the surface when a commercial Hopcalite was crystallized at high temperatures. This surface potassium was found to be responsi-

[1] To whom correspondence should be addressed.



0021-9517/91 $3.00

ble for the loss of activity of the catalyst after high-temperature treatments.

To obtain a more extended view on the surface properties of mixed oxides, we have studied mixed oxides of Cu, Co, and Mn by using XPS, Auger electron spectroscopy (AES), X-ray diffraction (XRD), and CO oxidation activity measurement. The importance of surface characterization on the understanding of catalysis is demonstrated.

## EXPERIMENTAL

### *Preparation of Catalysts*

Mixed oxides $MnCuCoO_x$, $MnCuO_x$, $MnCoO_x$, $CuCoO_x$, and $CuCo_2O_x$ were prepared by using a cold ethanol coprecipitation method developed earlier (*22*). $Co(NO_3)_2 \cdot 6H_2O$ (Merck, 99%), $Cu(NO_3)_2 \cdot 3H_2O$ (Riedel de Haen, 99%), and $Mn(NO_3)_2 \cdot 4H_2O$ (Merck, 98.5%) in selected ratios were first dissolved in ethanol (95%) to make a solution of total metal concentration 0.1 *M*. The solution was then sprayed into a beaker of cold ethanol (−30°C) saturated with $NH_3$ to allow rapid precipitation. The precipitate was filtered, dried at 100°C overnight, ground into a fine powder, and calcined in air at 500°C for 12 h.

Single oxides CuO and $Co_3O_4$ were prepared from their nitrate solutions (0.1 *M*) by conventional aqueous precipitation with ammonia water. The pH value was kept constant at 10.5 for $Co_3O_4$ and at 6.0 for CuO preparation. The precipitate was filtered, dried at 100°C overnight, ground into a fine powder, and air calcined at 500°C for 4 h. $MnO_2$ was obtained as a commercial product (Strem, activated).

### *Characterizations*

Catalysts were examined by XRD (Siemens D500 with Cu$K\alpha$ X-ray) for phase identification, by nitrogen adsorption for BET surface area measurement, and by inductively coupled plasma atomic emission spectroscopy (ICP–AES, Kontron Plasmakon S-35) for cation composition analysis.

XPS was performed on a VG Microlab MK III with a spherical sector analyzer operated in the constant pass energy (20 eV) mode. Al$K\alpha$ X-ray was used for all oxides and Mg$K\alpha$ was used in addition for $MnCuCoO_x$. The oxide powder was pressed onto a piece of indium foil (99.999%), which was grounded to the spectrometer in the examination. No electron flood gun was used. Surface cation compositions were calculated using the sensitivity factors provided by the manufacturer. The sensitivity factors are 13.62, 15.87, and 6.28 for Mn 2*p*, Cu $2p_{3/2}$, and Co $2p_{1/2}$ peaks, respectively. To calculate molar compositions, peak areas are divided by their individual sensitivity factors.

AES was also employed to determine the surface cation composition. A Perkin–Elmer PHI-590AM with a cylindrical mirror analyzer was used, and a 3-keV electron beam was used for the excitation. The powder sample was similarly prepared on a piece of In foil as in XPS studies, but in a more dispersed form to obtain a better electric contact. The cation composition was calculated by using the built-in computer program after a multiscan of Mn2, Co2, and Cu1 LMM Auger peaks.

### *CO Oxidation*

Catalytic activities of the oxides were studied in flow reaction of CO (0.5 vol%) in air at 100°C. The total flow rate was 40 ml/min. Products were analyzed on-line using a gas chromatograph with a Carbosieve S-II column. Before reaction, the catalyst was pretreated in flowing oxygen at 300°C for 30 min and at 450°C for 10 min to drive away molecules preadsorbed from the atmosphere. A suitable amount of catalyst was used to give a steady-state conversion of about 10% such that the areal activity could be calculated directly by making the assumption of a differential reactor.

## RESULTS

### *Conventional Characterizations and CO Oxidation Activity*

Table 1 compares the BET surface areas, the CO oxidation activity, the bulk composi-

TABLE 1

Results of XRD, BET Surface Area, CO Oxidation Activity, and Cation Composition Measurements

| Catalyst | BET surface area ($m^2/g$) | Activity[a] $\left(\frac{10^{-5}\text{ mole}}{m^2\text{ min}}\right)$ | Cation composition | | | | | | Phase |
|---|---|---|---|---|---|---|---|---|---|
| | | | Mother solution | | | Bulk[b] | | | |
| | | | Mn | Cu | Co | Mn | Cu | Co | |
| $MnCuCoO_x$ | 2.1 | 0.4 | 0.33 | 0.33 | 0.33 | 0.34 | 0.33 | 0.33 | Spinel $MnCuCoO_4$<br>Tenorite CuO (trace) |
| $MnCuO_x$ | 2.5 | 0.5 | 0.50 | 0.50 | | 0.52 | 0.48 | | Spinel $Cu_{1.5}Mn_{1.5}O_4$<br>Bixbyite $Mn_2O_3$ (weak)<br>Tenorite CuO (trace) |
| $CuCoO_x$ | 2.6 | 1.7 | | 0.50 | 0.50 | | 0.49 | 0.51 | Spinel $CuCo_2O_4$<br>Tenorite CuO |
| $CuCo_2O_x$ | 2.9 | 1.9 | | 0.33 | 0.67 | | 0.31 | 0.69 | Spinel $CuCo_2O_4$<br>Tenorite CuO (weak) |
| $MnCoO_x$ | 3.0 | | 0.50 | | 0.50 | 0.52 | | 0.48 | Possibly spinel $Co_3O_4$, spinel $MnCo_2O_4$, and bixbyite $Mn_2O_3$ |
| $Co_3O_4$ | 15.1 | 1.8 | | | | | | | Spinel $Co_3O_4$ |
| CuO | 0.6 | 1.7 | | | | | | | Tenorite CuO |
| $MnO_2$ | 90.5 | 0.08 | | | | | | | $MnO_{1.88}$ (weak) |

[a] CO oxidation activity at 100°C, 0.5 vol% CO in air, 40 ml/min.
[b] By ICP–AES.

tions of metal ions, and the crystallographic phases of the oxides. X-ray diffraction patterns of the mixed oxides are given in Fig. 1. As can be seen in Table 1, single and mixed oxides of Cu and Co were most active, while the activity of $MnO_2$ was one order of magnitude lower. Mixed oxides containing Mn were also considerably less active than the Mn-free oxides. The metal compositions of the final oxides were close to that of their mother solutions. Single oxides $Co_3O_4$ and CuO exhibited clean XRD patterns of spinel $Co_3O_4$ and tenorite CuO, respectively. Commercial $MnO_2$ is usually non-stoichiometric (*23*). The $MnO_2$ used in this study showed a very weak XRD pattern of $MnO_{1.88}$ (*24*).

On the crystallographic structures of the mixed oxides, the spinel phase was detected in most samples. However, none of them was structurally pure. $MnCuCoO_x$ was predominantly a spinel accompanied by a trace amount of tenorite CuO. By using a physical mixture of $MnCuCoO_x$ and CuO as an external reference, the amount of tenorite CuO in $MnCuCoO_x$ was estimated to be about 1%. The thermal stability of $MnCuCoO_x$ spinel was studied by further calcining the oxide in air at 700, 900, and 1000°C for 2 h separately. The spinel XRD pattern was sharpened after high-temperature calcination, but the tenorite phase still represented about 1% of the material. This indicates that $MnCuCoO_x$ spinel is stable up to 1000°C in air. Table 2 gives the diffraction data of spinel $MnCuCoO_x$, from which its unit cell length is calculated to be 8.20 ± 0.01 Å. Upon calcination at 1100°C, however, the oxide melted.

Coexistence of tenorite CuO in copper cobalt mixed oxides was not avoided even in the case of $CuCo_2O_x$, which has the cation stoichiometry for spinal $CuCo_2O_4$. The preparation of single-phase spinal $CuCo_2O_4$ requires special efforts (*25, 26*) and the structure is unstable at 400°C or above (*26*). For $MnCuO_x$, spinel $Cu_{1.5}Mn_{1.5}O_4$ was the major component, accompanied by bixbyite

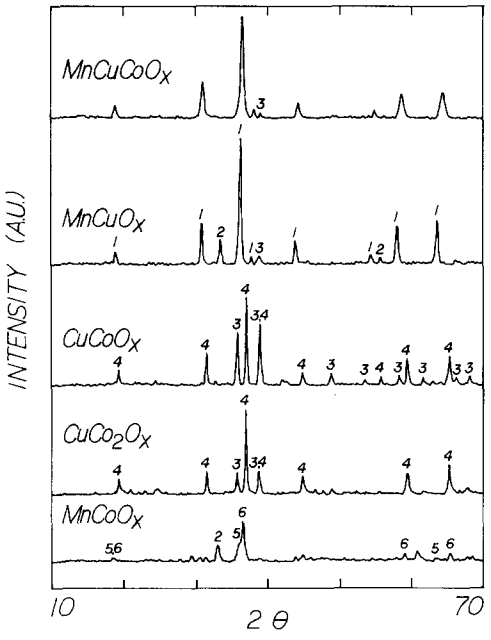


FIG. 1. X-ray diffraction patterns of $MnCuCoO_x$, $MnCuO_x$, $CuCoO_x$, $CuCo_2O_x$, and $MnCoO_x$(Cu$K\alpha$). "1" marks spinel $Cu_{1.5}Mn_{1.5}O_4$ peaks (JCPDS 35-1172), "2" marks bixbyite $Mn_2O_3$ peaks (JCPDS 24-0508), "3" marks tenorite CuO peaks (JCPDS 5-0661), "4" marks spinel $CuCo_2O_4$ peaks (JCPDS 1-1155), "5" marks spinel $MnCo_2O_4$ peaks (JCPDS 23-1237), and "6" marks spinel $Co_3O_4$ peaks (JCPDS 9-0418).

$Mn_2O_3$ and tenorite CuO in smaller amounts. The presence of three phases indicates that the sample was not at thermodynamic equilibrium (*27*). $MnCoO_x$ showed a weak and complex XRD pattern. A computer search suggested the possible inclusion of spinel $Co_3O_4$, spinel $MnCo_2O_4$, and bixbyite $Mn_2O_3$.

TABLE 2

X-Ray Diffraction Data of Spinel $MnCuCoO_x$

| *d*-Spacing (Å) | hkl | Relative intensity |
|---|---|---|
| 4.71 | 111 | 12 |
| 2.891 | 220 | 32 |
| 2.467 | 311 | 100 |
| 2.360 | 222 | 6 |
| 2.046 | 400 | 16 |
| 1.673 | 422 | 9 |
| 1.576 | 511,333 | 37 |
| 1.449 | 440 | 37 |

### *Surface Characterization by XPS and AES*

Table 3 summarizes the results of surface characterization by XPS and AES. Some X-ray photoelectron spectra are given in Fig. 2. In all studies, Mn, Cu, Co, O, C, and In were the only elements observed. No foreign elements, especially K, were present in a detectable amount. Potassium is a known poison in a commercial Mn–Cu Hopcalite (*21*). The oxides were X-ray stable. Pre-exposing them to X-ray radiation for 30 min did not result in any detectable difference in their XP spectra. All binding energy data reported in Table 3 have been adjusted against the C 1*s* peak standardized at 284.6 eV (*28*). With Al$K\alpha$ radiation, the Mn 2*p* peaks of $MnCuCoO_x$ were superimposed with the Cu $L_3M_{23}M_{45}$ Auger peak at 648 eV, thus making the quantification less accurate. This overlap was avoided by using Mg$K\alpha$ radiation, as can be seen in Fig. 2.

Several features are found in Table 3 and Fig. 2: (1) The results of XPS measurements on $MnCuCoO_x$ by using Al$K\alpha$ and Mg$K\alpha$ were in reasonable agreement with each other. (2) Surface cation compositions as measured by XPS and AES were in reasonable agreement too. (3) There was a strong surface enrichment of Mn over Cu and Co, and a surface enrichment of Cu over Co. (4) All Mn-containing mixed oxides exhibited a constant binding energy of 461.8 ± 0.1 eV for the Mn $2p_{3/2}$ peak. (5) On $CuCoO_x$ and $CuCo_2O_x$, the Cu $2p_{3/2}$ peak was at 933.7 ± 0.1 eV with a broad shake-up satellite peak about 8 eV higher. On all Mn-containing mixed oxides, the Cu $2p_{3/2}$ main peak shifted slightly toward lower binding energies and a sharp new peak appeared at 930.8 ± 0.1 eV with no appearance of new satellite peaks. (6) The positions of Co $2p_{3/2}$ peaks of different mixed oxides scattered more widely than that of Mn and Cu. In general, the Mn-

TABLE 3

Results of Surface Characterization by XPS[a] and AES

| Catalyst | $2p_{3/2}$ Binding energy[c] (eV) | | | Cation composition | | | | | |
|---|---|---|---|---|---|---|---|---|---|
| | Mn | Cu | Co | Surface[d] | | | Bulk[e] | | |
| | | | | Mn | Cu | Co | Mn | Cu | Co |
| $MnCuCoO_x$ | 641.8 | 930.8, 933.3 | 780.1(+7) | 0.54 | 0.33 | 0.14 | 0.34 | 0.33 | 0.33 |
| $MnCuCoO_x$[b] | 641.8 | 930.7, 933.1 | 780.3(+6) | 0.59 (0.48) | 0.27 (0.36) | 0.14 (0.16) | 0.34 | 0.33 | 0.33 |
| $MnCuO_x$ | 641.8 | 930.8, 933.6 | | 0.63 (0.67) | 0.37 (0.33) | | 0.52 | 0.48 | |
| $CuCoO_x$ | | 933.7 | 779.4(+10) | | 0.66 (0.67) | 0.34 (0.33) | | 0.49 | 0.51 |
| $CuCo_2O_x$ | | 933.8 | 779.8(+10) | | 0.60 (0.64) | 0.40 (0.36) | | 0.31 | 0.69 |
| $MnCoO_x$ | 641.9 | | 780.4(+6) | 0.74 | | 0.26 | 0.52 | | 0.48 |

[a] Al$K\alpha$ radiation except footnote *b*.
[b] Mg$K\alpha$ radiation.
[c] Values in parentheses are the separation of the satellite peak from the main peak.
[d] Values in parentheses were obtained by AES, others by XPS.
[e] By ICP–AES.

containing oxides showed higher Co $2p_{3/2}$ values than that of Mn-free oxides, but the difference was only about 0.5 eV. A clear difference between the Mn-containing oxides and the Mn-free oxides was on the position of the satellite peak. In the presence of Mn, the satellite peak of Co $2p_{3/2}$ was about 6 to 7 eV higher than the main peak, while in the absence of Mn, the Co satellite peak was separated from the main peak by about 10 eV. The last two observations suggest the internal reduction of Cu and Co ions by Mn ions as discussed below.

## DISCUSSION

### *Determination of Oxidation States of Surface Mn, Cu, and Co*

XPS is best known for its capability in disclosing the chemical states of a surface. On manganese oxides, $Mn^{4+}$ of $MnO_2$ has a $2p_{3/2}$ binding energy of 642 ± 0.2 eV, while $Mn^{3+}$ of $Mn_2O_3$ has a $2p_{3/2}$ at 641.3 eV (*28*). As can be seen in Table 3, the Mn $2p_{3/2}$ peaks of Mn-containing oxides were all at 641.8 ± 0.1 eV. This value is slightly lower than that of $Mn^{4+}$, but significantly higher than that of $Mn^{3+}$, suggesting that the average oxidation state of surface Mn is close to 4+ in all Mn-containing oxides studied.

$Cu^+$ and $Cu^{2+}$ on copper oxides are easily distinguishable in XPS. $Cu^{2+}$ is paramagnetic. Its $2p_{3/2}$ peak is at 933.5 ± 0.3 eV, and is accompanied by a strong shake-up satellite peak about 9 eV higher (*28, 29*). $Cu^+$ is diamagnetic. It has no shake-up satellite peak. The $2p_{3/2}$ peak of $Cu^+$ in $Cu_2O$ is at 932.2 ± 0.3 eV (*25, 26*). The sharp Cu $2p_{3/2}$ peak at 930.8 eV in Mn-containing oxides could be attributed to either metallic Cu or $Cu^+$. Metal Cu and $Cu_2O$ have their $2p_{3/2}$ peaks almost identical to each other, in both position and shape (*30, 31*). However, the two Cu species can be distinguished by examining their $L_3M_{45}M_{45}$ Auger peaks. Metallic Cu has a very sharp $L_3M_{45}M_{45}$ Auger peak with its full width at half maximum (FWHM) about 1 eV, while $Cu^+$ has a broad $L_3M_{45}M_{45}$ Auger peak with its FWHM over 2 eV (*30, 32*). In this study,

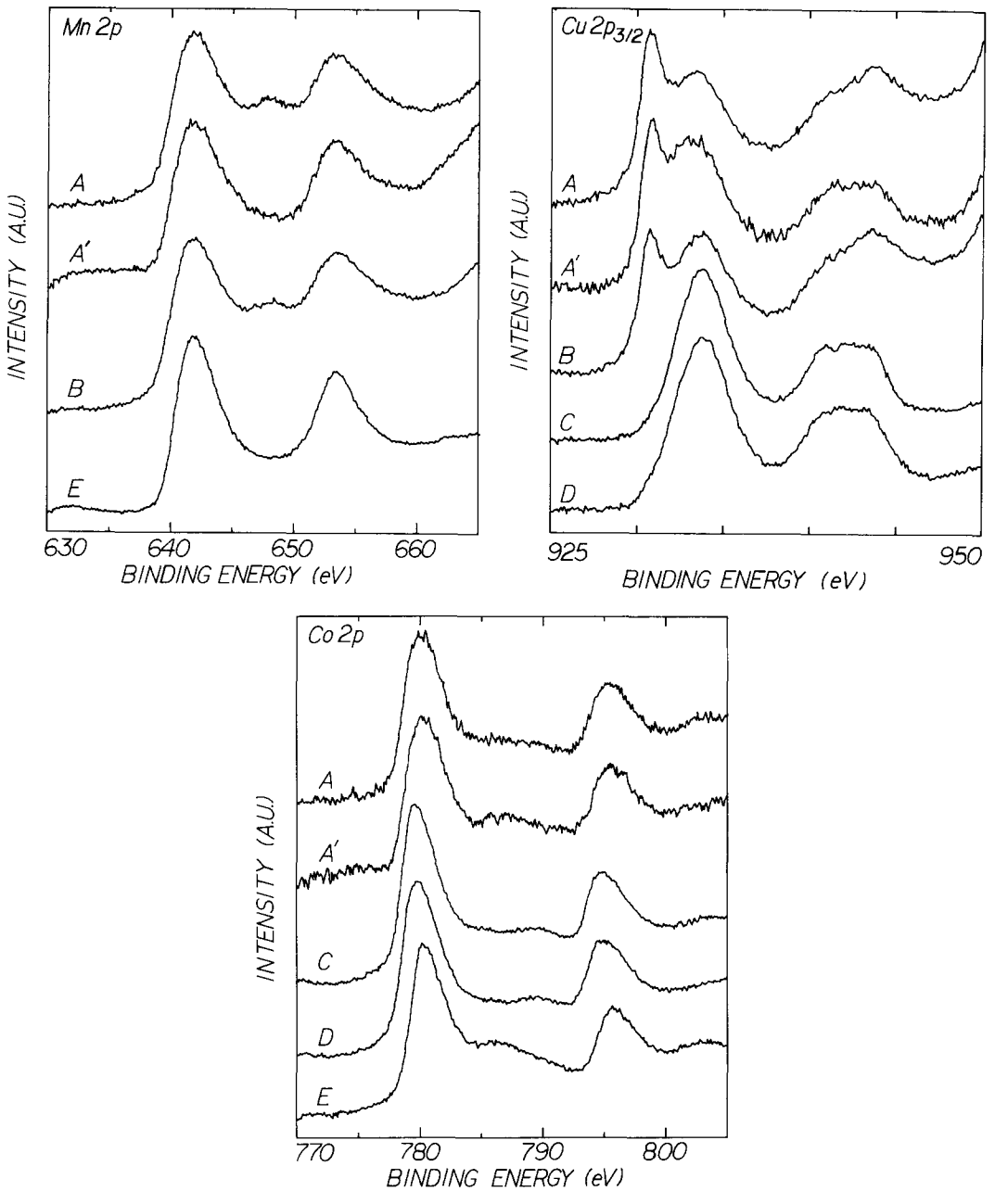


FIG. 2. X-ray photoelectron spectra of the mixed oxides. All spectra were obtained by using Al$K\alpha$ radiation except A'. A = $MnCuCoO_x$, A' = $MnCuCoO_x$ by Mg$K\alpha$, B = $MnCuO_x$, C = $CuCoO_x$, D = $CuCo_2O_x$, and E = $MnCoO_x$.

the Cu $L_3M_{45}M_{45}$ Auger peaks of both $MnCuCoO_x$ and $MnCuO_x$ were found to be broad, with their FWHM over 2 eV, thus suggesting the presence of $Cu^+$ but not metallic Cu at the surface.

As can be seen in Table 3 and Fig. 2, both $Cu^{2+}$ and $Cu^+$ were present on the Mn-containing mixed oxides, but there were only $Cu^{2+}$ on $CuCoO_x$ and $CuCo_2O_x$. Note that the $Cu^+$ in $MnCuCoO_x$ and $MnCuO_x$

had a $2p_{3/2}$ at 930.8 eV, about 1.4 eV lower than that of $Cu^+$ in $Cu_2O$. This negative chemical shift seems to be related to the local environment of $Cu^+$. A similar phenomenon has been observed on spinel $CuMg_{0.5}Mn_{1.5}O_4$ (*33*) and $CuMn_2O_4$ (*20, 21*), and has been interpreted by the higher negative charge of the four oxygen ions of the $CuO_4$ tetrahedron (*33*). The interpretation consequently suggests that $Cu^+$ ions occupy tetrahedral sites only.

XRD results revealed that $MnCuCoO_x$ was predominantly a spinel, thus an easy guess of the material would be $Cu^{2+}Mn^{3+}Co^{3+}O_4$. However, $Cu^+$ was suggested by XPS at the surface of $MnCuCoO_x$. The presence of $Cu^+$ would require some Mn or Co ions to exist in an oxidation state higher than 3+. Since Co does not normally exist in an oxidation state higher than 3, Mn is considered responsible for the presence of $Cu^+$. This argument is also supported by the fact that the presence of Co in $CuCoO_x$ and $CuCo_2O_x$ did not cause Cu to stay in the monovalent state, while $Cu^+$ was found in $MnCuO_x$ (Table 3 and Fig. 2). Note that the oxidation state of Cu in the starting material $Cu(NO_3)_2 \cdot 3H_2O$ was 2+, and no reduction was employed in the preparation of the oxide. An internal reduction of $Cu^{2+}$ must have occurred. $Mn^{3+}$ is therefore considered a strong reducing agent and an internal redox reaction

$$Cu^{2+} + Mn^{3+} \rightarrow Cu^+ + Mn^{4+}$$

could have occurred. Indeed, $Cu^+$(tet)-$Mn^{4+}$(oct) has been reported to be the most stable configuration in Cu–Mn-containing spinels (*27*). An average oxidation state close to 4+ found for surface Mn on $MnCuCoO_x$ is also in agreement with this explanation.

A similar reduction of Co by Mn was also observed. The main peak of Co $2p_{3/2}$ is not sensitive to the change in the oxidation state, but significant shifts of its shake-up satellite peak have been reported (*34, 35*). The weak Co $2p_{3/2}$ satellite has been found to be about 10 eV higher than its main peak over $Co_3O_4$, while the separation is only about 6 eV over CoO (*34, 35*). As can be seen in Table 2, whenever Mn was present, the Co $2p_{3/2}$ peaks showed a satellite separation of about 6 eV, similar to that of $Co^{2+}$ on CoO. In the absence of Mn, the Co peaks were 10 eV apart, just like $Co_3O_4$. This correlation suggests that the presence of Mn also results in the reduction of Co, possibly through an internal redox reaction

$$Mn^{3+} + Co^{3+} \rightarrow Mn^{4+} + Co^{2+}.$$

*Surface Enrichment*

Although mixed oxides used in this study were not single-phase compounds and therefore not ideal for segregation studies, all XPS results showed a general trend of surface enrichment in the order Mn > Cu > Co. Surface and grain boundary segregation in ceramic oxides has been studied intensively (*36–38*) and has found many engineering applications in advancing electronic and magnetic ceramic materials (*39*). However, the segregation in mixed oxide catalysts, which are often non-stoichiometric and structurally poorly defined, has not been studied much. Segregation in mixed oxides of transition metals is highly complicated. It has been shown that the segregation is related to the size of the segregating ion, which depends strongly on its oxidation state, the electric charge and the concentration of defects at the surface, the structure of the surface, and the gas atmosphere the surface exposes to (*1, 36–38*). As a result of surface enrichment, surface restructuring, and even the formation of a secondary phase at the surface may occur (*1, 40*).

Table 4 summarizes some literature data on surface segregation in mixed oxides of the first-row transition metals. Most studies were on the segregation of doped foreign elements, or solutes, at concentrations well below their solubility limits in the host oxide. On multicomponent oxidic compounds, Haber *et al.* (*44*) reported the absence of segregation on spinel $CoCr_2O_4$, but enrichment of one constituent cation over another

TABLE 4

Some Literature Data on the Surface Enrichment in Mixed Oxides of the First-Row Transition Metals

| Matrix oxide | Structure | Surface-enriched element | Analysis method[a] | Reference |
|---|---|---|---|---|
| NiO | Rocksalt | Mn>Fe>Co | Calc. | (*36*) |
| NiO | Rocksalt | Ti>Cr | STEM/EDS | (*41*) |
| NiO | Rocksalt | Cr | AES,SIMS | (*42, 43*) |
| CoO | Rocksalt | Cr | XPS | (*44*) |
| ZnO | Wurtzite | Cd | | (*40*) |
| $(Fe,Cr)_2O_3$ | Corundum | Cr | AES | (*45*) |
| $CoCr_2O_4$ | Spinel | — | XPS | (*44*) |
| $CuCr_2O_4$ | Spinel | Cu | ISS | (*46*) |
| $CuMn_2O_4$ | Spinel | Mn | XPS | (*20*) |
| $Cu_{0.5}Fe_{2.5}O_4$ | Spinel | Cu | XPS | (*33*) |
| $(Ni,Zn)Fe_2O_4$ | Spinel | Mn | | (*40*) |
| $(Mn,Zn)Fe_2O_4$ | Spinel | Ti | AES | (*40*) |
| $MnCuCoO_x$ | Spinel | Mn>Cu>Co | XPS,AES | This work |

[a] AES, Auger electron spectroscopy; Calc., calculated; ISS, ion scattering spectroscopy; SIMS, secondary ion mass spectrometry; STEM/EDS, scanning transmission electron microscopy with X-ray energy dispersive analysis; XPS, X-ray photoelectron spectroscopy.

at the surface was observed on spinel $Cu_{0.5}Fe_{2.5}O_4$ (*33*), $CuCr_2O_4$ (*46*), and $CuMn_2O_4$ (*20*). A depletion of Zn from the surface of spinel $Mn_{0.50}Zn_{0.42}Fe_{2.08}O_4$ was also reported (*47*).

In many cases the dominant factor determining the segregation is the size of the segregating cation, and the larger the size, the stronger the enrichment at the surface (*36*). This is, however, not the case for mixed oxides of Mn, Cu, and Co studied here, because the most enriched $Mn^{4+}$ has the smallest size among all cations present at the surface. The determinant factor is probably the gas atmosphere instead. Oxygen binding energies at the surfaces of $Co_3O_4$, CuO, and $MnO_2$ have been reported to be 67, 75, and 84 kJ/mole, respectively (*2*). A higher surface oxygen binding energy would mean a more stable oxide surface. The mixed oxides were calcined in air. The oxidative atmosphere would therefore attract Mn more over Cu and Co to the surface, thus resulting in the enrichment of Mn. Similarly, over mixed oxides of Cu and Co, Cu was more attracted to the surface. It is very likely that the segregation caused by differential attraction of cations by surface oxygen and the above discussed internal redox reaction between cations are interrelated.

For $CuCoO_x$ and $CuCo_2O_x$, although their bulk Cu/Co ratios are very different from each other, all surface composition measurements seem to suggest a common Cu/Co stoichiometry of 2 at their surfaces. This is an indication of possible formation of a surface compound. There is indeed a known bulk oxide $Cu_2CoO_3$ (*48*). However, since only $Cu^{2+}$ and no $Cu^+$ was detected at the surfaces of $CuCoO_x$ and $CuCo_2O_x$, the assumption of formation of a surface compound $Cu_2CoO_3$ would require Co at the surface to be divalent too. This, however, contradicts our XPS observation. The possibility of a surface compound formation on Cu–Co oxides would be an interesting area for additional research.

*CO Oxidation Activity*

The results that CuO and $Co_3O_4$ were about equally active and were one order of magnitude more active than $MnO_2$ is in agreement with literature reports (*2*). The activity data reported in Table 1 also fit well with literature data (*2*). The activity data show no clear correlation with the bulk structure. Instead, the difference in CO oxidation activity among different oxides can be well explained by two surface phenomena, the enrichment of Mn over Cu and Co at the surface, and the reduction of Cu and Co ions by Mn ions. As discussed above, Mn was strongly enriched at the surface over Co and Cu. Since manganese oxide was least active among the three single oxides, the enrichment of Mn over Cu and Co would result in a lowering of the overall activity of the mixed oxides. Cu was enriched over Co in $CuCoO_x$ and $CuCo_2O_x$. However, since CuO and $Co_3O_4$ were about equally active, the surface enrichment did not cause a difference in overall activity and the mixed oxides were about equally active as CuO and $Co_3O_4$.

Assuming the activity of a mixed oxide is the summation of the activities of its component oxides present at the surface, we can calculate the overall activities of the mixed oxides and eompare them with experimental data. In the cases of $CuCoO_x$ and $CuCo_2O_x$, the calculated values ($1.7 \times 10^{-5}$ mole/m$^2$ min for both) fit quite well with experimental data as expected. However, for $MnCuCoO_x$ and $MnCuO_x$, the calculated values (0.8 and $0.7 \times 10^{-5}$ mole/m$^2$ min, respectively) are significantly higher than the experimental data. This can be explained by the fact that Cu and Co ions are partially reduced by Mn ions at the surfaces of the mixed oxides, thus the overall activities calculated based on that of the fully oxidized component oxides are over estimated.

## CONCLUSIONS

It is demonstrated that surface composition of a mixed oxide can be very different from its bulk composition. The coexistence of different metal ions in a mixed oxide may result in internal redox reactions and possibly a significant change in its overall catalytic properties.

In the case of CO oxidation, CuO and $Co_3O_4$ are found to be much more active than $MnO_2$. Over the mixed oxides, however, Mn tends to migrate to the surface, resulting in a lowering of the overall activity. XPS data also suggest that Co and Cu ions at the surface are partially reduced by Mn ions. This also explains in part the low activities of the Mn-containing mixed oxides. For mixed oxides of Cu and Co, Cu is enriched at the surface. However, their activities are comparable to that of CuO and $Co_3O_4$, because both Cu and Co in the mixed oxides are in their fully oxidized states and the two single oxides are about equally active.

## ACKNOWLEDGMENTS

The National Science Council of the Republic of China is greatly appreciated for supporting this work. The authors are in debt to Mr. Shean-Ren Horng and Miss Rita Hwang of Industrial Technology Research Institute, Hsinchu, Taiwan, for collecting XPS data.

## REFERENCES

1. Kung, H. H., "Transition Metal Oxides: Surface Chemistry and Catalysis," Studies in Surface Science and Catalysis, Vol. 45, Elsevier, Amsterdam, 1989.
2. Boreskov, G. K., *in* "Catalysis Science and Technology" (J. R. Anderson and M. Boudart Eds.), Vol. 3, Chap. 2. Springer-Verlag, Berlin, 1982.
3. Machida, M., Eguchi, K., and Arai, H., *J. Catal.* **120,** 377 (1989).
4. Merrill, D. R., and Scalione, C. C., *J. Am. Chem. Soc.* **43,** 1982 (1921).
5. Kummer, J. T., *Prog. Energy Combust. Sci.* **6,** 177 (1980).
6. Taylor, K. C., *in* "Catalysis Science and Technology" (J. R. Anderson and M. Boudart Eds.), Vol. 5, Chap. 2. Springer-Verlag, Berlin, 1984.
7. Angelov, S., Mehandjiev, D., Piperov, B., Zarkov, V., Terlecki-Baricevic, A., Jovanovic, D., and Jovanovic, Z., *Appl. Catal.* **16,** 431 (1985).
8. Haruta, M., Yamada, N., Kobayashi, T., and Iijima, S., *J. Catal.* **115,** 301 (1989).
9. Brittan, M. I., Bliss, H., and Walker, C. A., *AIChE J.* **16,** 305 (1970).
10. Kanungo, S. B., *J. Catal.* **58,** 419 (1979).

11. Panayotov, D., Khristova, M., and Mehandjiev, D., *Appl. Catal.* **34,** 49 (1987).
12. Severino, F., and Laine, J., *Ind. Eng. Chem. Prod. Res. Dev.* **22,** 396 (1983).
13. Voorkoeve, R. J. H., Johnson Jr., D. W., Remeika, J. P., and Gallagher, P. K., *Science* **195,** 827 (1977).
14. Yu Yao, Y. F., *J. Catal.* **36,** 266 (1975).
15. Yu Yao, Y. F., and Kummer, J. T., *J. Catal.* **46,** 388 (1977).
16. Isupova, L. A., Yu Aleksandrov, V., Popovskii, V. V., Balashov, V. A., Davydov, A. A., Budneva, A. A., and Kryukova, N. N., *React. Kinet. Catal. Lett.* **31,** 195 (1986).
17. Angelov, S. A., and Bonchev, R. P., *Appl. Catal.* **24,** 219 (1986).
18. Yu Yao, Y. F., *J. Catal.* **39,** 104 (1975).
19. Lamb, A. B., and Vail, W. E., *J. Am. Chem. Soc.* **47,** 123 (1925).
20. Yoon, C., and Cocke, D. L., *J. Catal.* **113,** 267 (1988).
21. Veprek, S., Cocke, D. L., Kehl, S., and Oswald, H. R., *J. Catal.* **100,** 250 (1986).
22. Yang, B. L., Cheng, D. S., and Lee, S. B., *Appl. Catal.*, **70,** 161 (1991).
23. M. Windholz, Ed., "The Merck Index," 9th ed., p. 744. Merck & Co., Rahway, NJ, 1976.
24. JCPDS file 5-0673, International Centre for Diffraction Data, 1601 Park Lane, Swarthmore, PA, 1983.
25. Angelov, S., Zhecheva, E., Petrov, K., and Menandjiev, D., *Mat. Res. Bull.* **17,** 235 (1982).
26. Petrov, K., and Markov, L., *J. Mat. Sci.* **20,** 1211 (1985).
27. Vandenberghe, R. E., *Phys. Status Solidi A* **50,** K85 (1978).
28. Wagner, C. D., Riggs, W. M., Davis, L. E., and Moulder, J. F., "Handbook of X-ray Photoelectron Spectroscopy." Perkin–Elmer Corp., Physical Electronics Div., Eden Prairie, MN, 1979.
29. McIntyre, N. S., and Cook, M. G., *Anal. Chem.* **47,** 2208 (1975).
30. Haber, J., Machej, T., Ungier, L., and Ziolkowski, J., *J. Solid State Chem.* **25,** 207 (1978).
31. Castro, V. D., Furlani, C., Gargano, M., and Rossi, M., *Appl. Surf. Sci.* **28,** 270 (1987).
32. Braithwaite, M. J., Joyner, R. W., and Roberts, M. W., *Faraday Disc. Chem. Soc.* **60,** 89 (1976).
33. Brabers, V. A. M., *Mat. Res. Bull.* **18,** 861 (1983).
34. Chuang, T. J., Brundle, C. R., and Rice, D. W., *Surf. Sci.* **59,** 413 (1976).
35. Moyes, R. B., and Roberts, M. W., *J. Catal.* **49,** 216 (1977).
36. Kingery, W. D., *Pure Appl. Chem.* **56,** 1703 (1984).
37. Burggraaf, A. J., and Winnubst, A. J. A., *in* "Surface and Near-Surface Chemistry of Oxide Materials" (J. Nowotny and L. C. Dufour, Eds.), Chap. 10. Elsevier, Amsterdam, 1988.
38. Wynblatt, P., and McCune, R. C., *in* "Surface and Near-Surface Chemistry of Oxide Materials" (J. Nowotny and L. C. Dufour, Eds.), Chap. 6. Elsevier, Amsterdam, 1988.
39. L. M. Levinson, Ed., "Grain Boundary Phenomena in Electronic Ceramics," Advances in Ceramics, Vol. 1. Am. Ceram. Soc., Columbus, OH, 1981.
40. Bongers, P. F., and Franken, P. E. C., *in* "Grain Boundary Phenomena in Electronic Ceramics" (L. M. Levinson, Ed.), p. 38. Am. Ceram. Soc., Columbus, OH, 1981.
41. Notis, M. R., Bender, B., and Williams, D. B., *in* "Grain Boundary Phenomena in Electronic Ceramics" (L. M. Levinson, Ed.), p. 91. Am. Ceram. Soc. Columbus, OH, 1981.
42. Hirschwald, W., Sikora, J., and Stolze, F., *Surf. Interface Anal.* **7,** 155 (1985).
43. Bender, B., Williams, D. B., and Notis, M. R., *J. Am. Ceram. Soc.* **63,** 542 (1980).
44. Haber, J., Nowotny, J., Sikora, I., and Stoch, J., *Appl. Surf. Sci.* **17,** 324 (1984).
45. Kung, M. C., and Kung, H. H., *Surf. Sci.* **104,** 253 (1981).
46. Shelef, M., Wheeler, M. A. Z., and Yao, H. C., *Surf. Sci.* **47,** 697 (1975).
47. Sundahl Jr., R. C., Ghate, B. B., Holmes, R. J., and Pass, C. E., *in* "Advances in Ceramics" (L. M. Levinson Ed.), Vol. 1, p. 502, Am. Ceram. Soc., Columbus, OH, 1981.
48. JCPDS file 21-0288, International Centre for Diffraction Data, 1601 Park Lane, Swarthmore, PA, 1983.